JOURNAL OF COMPUTATIONAL PHYSICS **41**, 329–356 (1981)

On a Fourth Order Accurate Implicit Finite Difference Scheme for Hyperbolic Conservation Laws. II. Five-Point Schemes*

A. HARTEN AND H. TAL-EZER

Department of Mathematics, Tel-Aviv University, Tel-Aviv, Israel

Received July 9, 1979

This paper presents a family of two-level five-point implicit schemes for the solution of one-dimensional systems of hyperbolic conservation laws, which generalized the Crank–Nicholson scheme to fourth order accuracy (4–4) in both time and space. These 4–4 schemes are nondissipative and unconditionally stable. Special attention is given to the system of linear equations associated with these 4–4 implicit schemes. The regularity of this system is analyzed and efficiency of solution-algorithms is examined. A two-datum representation of these 4–4 implicit schemes brings about a compactification of the stencil to three mesh points at each time-level. This compact two-datum representation is particularly useful in deriving boundary treatments. Numerical results are presented to illustrate some properties of the proposed scheme.

1. INTRODUCTION

We consider here numerical solutions of a one-dimensional system of conservation laws

$$w_t + f(w)_x = 0. \tag{1.1}$$

where $w(x, t)$ is an m-vector of unknowns and $f(w)$ is a vector valued function of m components. The system (1.1) is said to be (strictly) hyperbolic when all eigenvalues $a_1(w),..., a_m(w)$ of the Jacobian matrix

$$A(w) = \text{grad}_w f \tag{1.2}$$

are real and distinct; the eigenvalues $a_k(w)$ are also referred to as characteristic speeds. Throughout this paper we denote by $v_j^n = v(j\Delta x, n\Delta t)$ a discrete approximation to solutions $w(x, t)$ of (1.1), where Δx and Δt are the space and time increments, respectively. We denote the CFL (Courant–Friedrichs–Lewy) number by $|\nu|$

$$|\nu| \equiv \frac{\Delta t}{\Delta x} \max |a_k(w)|. \tag{1.3}$$

* This report was prepared as a result of work performed under NASA Contract NAS1-14101 while the authors were in residence at ICASE, NASA Langley Research Center, Hampton, Va. 23665.

0021-9991/81/060329-28$02.00/0

The CFL number, which is the ratio of the maximal characteristic speed to the speed $\Delta x/\Delta t$ of the numerical mesh, is an important parameter in the numerical solution of hyperbolic problems.

This paper is a condensed version of the ICASE report [4] and is a sequel to [5], in which we have introduced a generalization of the Crank–Nicholson scheme to fourth order accuracy (in both time and space). In Section 2 we repeat the derivation of this scheme, which we denote by CN44: it is an implicit, unconditionally stable, nondissipative, two-leval three-point scheme (i.e., it uses three spatial mesh points at each level).

In Section 3 we analyze the solvability of the system of linear equations associated with three-point implicit schemes. We show that the system of linear equations associated with CN44 may become singular for $|\nu| \geqslant 1$. Consequently, CN44 can be applied only under the CFL restriction $|\nu| < 1$. In [5] we have also introduced a dissipative version of CN44 which is conditionally stable for $|\nu| \leqslant 1$. This dissipative version is particularly useful for numerical solutions of problems with strong but nonstiff dynamic features.

The singularity of the algebraic system associated with CN44 is due to its compact spatial discretization, which allows a mesh-oscillation eigenvector with a zero eigenvalue. This singularity can be overcome by enlarging the stencil of the 4–4 scheme to five spatial mesh points at each time-level (i.e., five-point schemes). In Section 4 we study a two-parameter family of five-point schemes and choose values of the parameters so that the pentadiagonal matrix associated with the scheme is nonsingular for all CFL numbers. We denote this scheme by FP44.

In Section 5 we describe an iterative technique for the solution of the system of linear equations associated with FP44. This iterative technique is more efficient than Gaussian elimination for $|\nu| < 4$ and has the practical advantage of easy implementation in a 2–4 Crank–Nicholson computer code. In Section 6 we study a two-datum representation of FP44 which results in a block tridiagonal system of linear equations. In Sections 7 and 8 we present some numerical results to demonstrate the performance of FP44.

We refer the reader who is interested in more background material to [5] and the references cited therein.

2. Numerical Background

One constructs an implicit Crank–Nicholson-type scheme for the solution of $w_t + f(w)_x = 0$ by replacing the integral in the relation

$$w^{n+1} = w^n + \int_t^{t+\Delta t} w_t \, dt \tag{2.1}$$

with a trapezoidal rule, i.e.,

$$w^{n+1} = w^n + \frac{\Delta t}{2} (w_t^n + w_t^{n+1}) + O((\Delta t)^3)$$

and then substituting $w_t = -f_x$ to obtain

$$w^{n+1} + \frac{\Delta t}{2} f_x^{n+1} = w^n - \frac{\Delta t}{2} f_x^n + O((\Delta t)^3). \tag{2.2}$$

To introduce spatial discretization we make use of the following finite difference operators:

$$\frac{1}{\Delta x} \mu\delta f = f_x + O((\Delta x)^2), \tag{2.3a}$$

$$\frac{1}{\Delta x} \frac{\mu\delta}{1 + \delta^2/6} f = f_x + O((\Delta x)^4) \tag{2.3b}$$

where μ and δ are the commonly used operators

$$\mu = \tfrac{1}{2}(T^{1/2} + T^{-1/2}), \qquad \delta = T^{1/2} - T^{-1/2};$$

T is the translation operator, $T^{\alpha} v(x) = v(x + \alpha\Delta x)$. Approximating f_x in (2.2) by (2.3a) and (2.3b) we obtain

$$v^{n+1} + \frac{\lambda}{2} \mu\delta f^{n+1} = v^n - \frac{\lambda}{2} \mu\delta f^n, \tag{2.4a}$$

$$(1 + \delta^2/6)\, v^{n+1} + \frac{\lambda}{2} \mu\delta f^{n+1} = (1 + \delta^2/6)\, v^n - \frac{\lambda}{2} \mu\delta f^n, \tag{2.4b}$$

respectively; here $\lambda = \Delta t/\Delta x$ and $f^l = f(v^l)$.

One may linearize the schemes in (2.4) by expanding f^{n+1} around v^n in the following way (see [1])

$$f^{n+1} = f^n + A^n(v^{n+1} - v^n) + O((\Delta t)^2). \tag{2.5}$$

Denoting $\Delta v^n = v^{n+1} - v^n$ we rewrite the linearized schemes in (2.4) in the computationally convenient Δ-formulation of Beam and Warming [2], (2.4a) and (2.4b) become, respectively

$$\text{CN22:} \qquad \left(1 + \frac{\lambda}{2} \mu\delta A^n\right) \Delta v^n = -\lambda\mu\delta f^n, \tag{2.6a}$$

$$\text{CN24:} \qquad \left(1 + \delta^2/6 + \frac{\lambda}{2} \mu\delta A^n\right) \Delta v^n = -\lambda\mu\delta f^n. \tag{2.6b}$$

Both schemes in (2.6) are unconditionally stable, nondissipative and second order accurate in the time variable. The scheme (2.6a), which we denote by CN22 is also second order in the space variable. The scheme (2.6b) is fourth order in the space variable and shall be referred to as CN24. Both schemes use a centered stencil of six points: three at level n and three at level $n + 1$.

In the first installment of this series we have described a fourth order accurate (in both space and time) generalization of the Crank–Nicholson scheme. This scheme, which we denote by CN44, can be easily derived from discretizing the integral in (2.1) by a trapezoidal rule with end corrections (see [3, p. 105])

$$w^{n+1} = w^n + \frac{\Delta t}{2}(w_t^n + w_t^{n+1}) + \frac{(\Delta t)^2}{12}(w_{tt}^n - w_{tt}^{n+1}) + O((\Delta t)^5) \tag{2.7a}$$

and then substituting $w_t = -f_x$, $w_{tt} = (Af_x)_x$ from the partial differential equation (1.1)

$$\begin{aligned} w^{n+1} &+ \frac{\Delta t}{2} f_x^{n+1} + \frac{(\Delta t)^2}{12}(A^{n+1} f_x^{n+1})_x \\ &= w^n - \frac{\Delta t}{2} f_x^n + \frac{(\Delta t)^2}{12}(A^n f_x^n)_x + O((\Delta t)^5). \end{aligned} \tag{2.7b}$$

To obtain fourth order accuracy in space we approximate f_x by (2.3c) and $(Af_x)_x$ by

$$(Af_x)_x = \frac{1}{(\Delta x)^2}\,\delta A \delta f + O((\Delta x)^2). \tag{2.7c}$$

Thus (2.7b) becomes

$$\begin{aligned} (1 + \delta^2/6)\, v^{n+1} &+ \frac{\lambda}{2}\mu\delta f^{n+1} + \frac{\lambda^2}{12}\delta A^{n+1}\delta f^{n+1} \\ &= (1 + \delta^2/6)\, v^n - \frac{\lambda}{2}\mu\delta f^n + \frac{\lambda^2}{12}\delta A^n \delta f^n. \end{aligned} \tag{2.8}$$

To linearize the scheme (2.8) and still preserve its temporal fourth order accuracy, we first obtain a second order accurate approximation $\hat{v}$ to the solution of (1.1) at level $n+1$

$$\hat{v} = v^{n+1} + O((\Delta t)^3). \tag{2.9a}$$

Then we expand f^{n+1} and A^{n+1} around $\hat{v}$ in the following way

$$f^{n+1} = \hat{f} + \hat{A}(v^{n+1} - \hat{v}) + O(\|v^{n+1} - \hat{v}\|^2) \equiv \tilde{f} + \hat{A}\Delta v^n + O((\Delta t)^6), \tag{2.9b}$$

$$A^{n+1} = \hat{A} + O((\Delta t)^3), \tag{2.9c}$$

where $\hat{A} = A(\hat{v})$, $\hat{f} = f(\hat{v})$, and $\tilde{f}$ denotes

$$\tilde{f} = \hat{f} + \hat{A}(v^n - \hat{v}) \tag{2.9d}$$

and as before $\Delta v^n = v^{n+1} - v^n$. Using this linearization we obtain the following Δ-form

$$\text{CN44:} \quad \left(1 + \delta^2/6 + \frac{\lambda}{2}\mu\delta\hat{A} + \frac{\lambda^2}{12}\delta\hat{A}\delta\hat{A}\right)\Delta v^n = -\frac{\lambda}{2}\mu\delta(f^n + \hat{f}) + \frac{\lambda^2}{12}\delta(A^n\delta f^n - \hat{A}\delta\hat{f}). \tag{2.10}$$

In the constant coefficient case

$$w_t + A w_x = 0, \qquad A = \text{constant} \tag{2.11}$$

CN44 becomes

$$\left(1 + \delta^2/6 + \frac{\lambda}{2}A\mu\delta + \frac{\lambda^2}{12}A^2\delta^2\right)\Delta v^n = -\lambda A\mu\delta v^n, \tag{2.12}$$

which is nondissipative and unconditionally stable; thus the linear stability of CN44 does not depend on the way $\hat{v}$ in (2.9a) is calculated. (2.12) has the same centered stencil of three points at level n and three points at level $n+1$ as CN22 and CN24. As this is the smallest stencil possible to obtain 4–4 accuracy we shall also refer to CN44 as a compact 4–4 scheme.

3. Solvability and Direct Factorization

The implicit schemes of Section 2 can be written in the form

$$Qv^{n+1} = Rv^n, \tag{3.1a}$$

where Q and R are finite difference operators with a support of three points.

$$(Qv)_j = b_j v_{j-1} + a_j v_j + c_j v_{j+1}, \tag{3.1b}$$

$$(Rv)_j = \hat{b}_j v_{j-1} + \hat{a}_j v_j + \hat{c}_j v_{j+1}. \tag{3.1c}$$

Throughout this paper we assume that the mesh points $1 \leqslant j \leqslant N$ are interior points and that $j = 0$ and $j = N+1$ are boundary points. The finite difference operator Q is represented by a matrix $Q_{i,j}$, which is block tridiagonal except for boundary terms. For periodic boundary conditions we have $v_0^l \equiv v_N^l$, $v_{N+1}^l \equiv v_1^l$ for $l \geqslant 0$, thus

$$Q = \begin{bmatrix} a_1 & c_1 & & & & b_1 \\ b_2 & & & & 0 & \\ & & b_i & a_i & c_i & \\ & 0 & & & & \\ & & & & & c_{N-1} \\ c_N & & & & b_N & a_N \end{bmatrix}; \qquad v = \begin{pmatrix} v_1 \\ \vdots \\ v_N \end{pmatrix}. \tag{3.1d}$$

We analyze now the scalar constant coefficient case where $b_j \equiv b$, $c_j \equiv c$, $a_j \equiv a$.

$$\text{CN22:} \quad b = -\frac{\nu}{4}, \qquad a = 1, \qquad c = \frac{\nu}{4},$$

$$\text{CN24:} \quad b = \frac{1}{12}(2 - 3\nu), \qquad a = \frac{2}{3}, \qquad c = \frac{1}{12}(2 + 3\nu), \tag{3.2b}$$

$$\text{CN44:} \quad b = \frac{1}{12}(2 - 3\nu + \nu^2), \qquad a = \frac{1}{6}(4 - \nu^2), \qquad c = \frac{1}{12}(2 + 3\nu + \nu^2), \tag{3.2c}$$

$$\hat{b} = c, \qquad \hat{a} = a, \qquad \hat{c} = b. \tag{3.2d}$$

It is easy to see that the matrix Q in (3.1d) is diagonally dominant (i.e., $|a| > |b| + |c|$) if and only if

$$\text{CN22:} \quad |\nu| < 2, \tag{3.3a}$$

$$\text{CN24:} \quad |\nu| < \tfrac{4}{3}, \tag{3.3b}$$

$$\text{CN44:} \quad |\nu| < 1. \tag{3.3c}$$

A diagonal dominant matrix Q is invertible and can be factored without pivoting into a product of a lower triangular matrix L and an upper triangular matrix U, i.e., $Q = LU$ (see [8, pp. 55–61]). However, diagonal dominance is only a sufficient condition for regularity of Q and direct LU factorization.

To analyze regularity let us evaluate the eigenvalues of Q. For simplicity let us assume $-\pi \leqslant x \leqslant \pi$, $\Delta x = 2\pi/N$, $x_j = -\pi + j\Delta x$, and we want to solve for v_j, $1 \leqslant j \leqslant N$. The mesh function

$$\{v^{(k)}\}_j = e^{ikj\Delta x} = e^{(i2\pi k/N)j} \qquad 1 \leqslant j \leqslant N$$

is an eigenvector of Q for all $1 \leqslant k \leqslant N$.

$$Qv^{(k)} = (be^{-i\xi} + a + ce^{i\xi})\, v^{(k)} \equiv q_k(\xi)\, v^{(k)}, \tag{3.4}$$

where $\xi = k\Delta x = 2\pi k/N$. The eigenvalues $q_k(\xi)$ are given by

$$\text{CN22:} \quad q_k(\xi) = 1 + i\frac{\nu}{2}\sin\xi, \tag{3.5a}$$

$$\text{CN24:} \quad q_k(\xi) = 1 - \frac{2}{3}\sin^2\frac{\xi}{2} + i\frac{\nu}{2}\sin\xi, \tag{3.5b}$$

$$\text{CN44:} \quad q_k(\xi) = 1 - \frac{1}{3}(2 + \nu^2)\sin^2\frac{\xi}{2} + i\frac{\nu}{2}\sin\xi. \tag{3.5c}$$

It follows that Q for CN22 and CN24 is always regular; however, for CN44, $q_k(\xi)=0$ for $\xi=\pi$, $|\nu|=1$. Thus, in the periodic case with even N, $v_j^{(N/2)}=e^{i\pi j}=(-1)^j$ is an eigenvector with a zero eigenvalue and Q is singular.

In [4, Appendix A] the stability of a direct LU factorization without pivoting for Crank–Nicholson type schemes is analyzed in the scalar constant coefficient case. It is shown there that the coefficient matrix of CN22 and CN24 can always be factored without pivoting and the solution algorithm is always stable (see also [9]). Although it is possible to factor CN44 for all $|\nu|<2$, it yields a stable solution algorithm only for $|\nu|<1$.

We remark that in the periodic case, R, the operator on the RHS of (3.1a) is the adjoint of Q, i.e., $R=Q^*$ and $r_k(\xi)=\bar{q}_k(\xi)$. Therefore, the singularity in CN44 can be "removed" by using a generalized inverse in solving the linear system associated with CN44. Numerical experiments, not reported in this paper, seem to confirm this observation.

In the next section we show how to remove this mesh oscillation singularity by enlarging the stencil of CN44 to five spatial mesh points.

4. Five-Point Schemes

We consider the following two-parameter family of 4–4 schemes in the constant coefficient case

$$\left\{1+\delta^2/6+\alpha\frac{\delta^4}{48}+\frac{\nu}{2}\mu\delta+\frac{\nu^2}{12}\left[(1-\beta)\,\delta^2+\beta(\mu\delta)^2\right]\right\}\Delta v^n=-\nu\mu\delta v^n \tag{4.1}$$

Since $\mu^2=1+\frac{1}{4}\delta^2$, we can rewrite (4.1) as

$$\left[\left(1+\delta^2/6+\frac{\nu}{2}\mu\delta+\frac{\nu^2}{12}\delta^2\right)+(\alpha+\beta\nu^2)\frac{\delta^4}{48}\right]\Delta v^n=-\nu\mu\delta v^n.$$

Thus (4.1) with $\alpha=\beta=0$ is CN44; since $\delta^4\Delta v^n=O(\Delta t(\Delta x)^4)$, (4.1) has 4–4 accuracy for all α and β. The Fourier symbol of (4.1) is

$$\left[1-\frac{1}{3}Y(2+\nu^2)+\frac{1}{3}Y^2(\alpha+\beta\nu^2)+i\frac{\nu}{2}\sin\xi\right](S-1)=-i\nu\sin\xi,$$

where $\xi=k\Delta x$, $0\leqslant\xi<\pi$, $Y=\sin^2(\xi/2)$, and S is the amplification factor of (4.1). The eigenvalues of the coefficient matrix Q are therefore

$$q(\xi,\nu)=1-\frac{1}{3}Y(2+\nu^2)+\frac{1}{3}Y^2(\alpha+\beta\nu^2)+i\frac{\nu}{2}\sin\xi. \tag{4.2}$$

The imaginary part of q vanishes at $\xi=0$ and $\xi=\pi$ ($Y=0$, $Y=1$), but $q(0,\nu)=1$, and

$$q(\pi,\nu)=\tfrac{1}{3}(1+\alpha)+\tfrac{1}{3}(\beta-1)\,\nu^2. \tag{4.3a}$$

Hence, the condition

$$\alpha>-1, \qquad \beta\geqslant 1 \tag{4.3b}$$

ensures regularity of the coefficient matrix. It is easily seen that

$$|q(\xi,\nu)|\geqslant\tfrac{1}{3}\min(1,1+\alpha), \qquad \alpha>-1. \tag{4.3c}$$

The amplification factor S of (4.1) is given by

$$S=\frac{\bar{q}(\xi,\nu)}{q(\xi,\nu)} \tag{4.4a}$$

thus,

$$|S|=1, \qquad S=e^{-i\phi(\xi,\nu)}, \tag{4.4b}$$

where

$$\phi(\xi,\nu)=2\tan^{-1}\left[\frac{(\nu/2)\sin\xi}{1-\frac{1}{3}Y(2+\nu^2)+\frac{1}{3}Y^2(\alpha+\beta\nu^2)}\right]. \tag{4.4c}$$

Hence, (4.1) is unconditionally stable for all choices of α and β. $\phi(\xi,\nu)$ is the numerical phase shift induced by (4.1) in a time-step Δt for an e^{ikx} wave. The exact phase shift induced by the solution operator of the differential equation in a Δt is $\phi_E=kA\Delta t=\nu\xi$. Expanding $\phi-\phi_E$ in a Taylor series for small ξ we get

$$\phi-\phi_E=-\frac{\nu\xi^5}{720}\,[\nu^4+5\nu^2(3\beta-1)+4+15\alpha]+O(\xi^7). \tag{4.5}$$

We observe that for the compact CN44, $\alpha=\beta=0$, we get

$$\phi-\phi_E=-\frac{\xi^5}{720}\,\nu(\nu^2-4)(\nu^2-1)+O(\xi^7) \tag{4.6a}$$

and indeed $\phi\equiv\phi_E$ for $|\nu|=1$ and $|\nu|=2$. However, to guarantee solvability we have $\alpha>-1$, $\beta\geqslant 1$, and therefore

$$|\phi-\phi_E|>\frac{|\nu\xi^5|}{720}\,|\nu(\nu^2-1)|\,(\nu^2+6)+O(\xi^7), \tag{4.6b}$$

which is always less accurate than (4.6a). In order to prevent ill-conditioning of the coefficient matrix one should not choose α too close to -1. We elect to choose $\alpha=0$,

$\beta = 1$ because of its computational simplicity. In this case $|q(\xi, \nu)| \geqslant \frac{1}{3}$ and the phase error is

$$\phi - \phi_E = \frac{\xi^5}{720} \nu(\nu^4 + 10\nu^2 + 4) + O(\xi^7). \tag{4.6c}$$

The pentadiagonal coefficient matrix of (4.1) with $\alpha = 0$, $\beta = 1$ is diagonally dominant for $|\nu| < -3 + \sqrt{17} \approx 1.123$. We remark that one can enlarge the domain of diagonal dominance by taking larger values of α and β but at the expense of increasing the phase error. Our numerical experiments indicate that a direct LU factorization without pivoting is possible for much larger values of CFL number.

Now we describe the proposed five-point scheme for nonlinear conservation laws:

$$\begin{aligned} &(1 + \delta^2/6)\, v^{n+1} + \frac{\lambda}{2} \mu\delta f^{n+1} + \frac{\lambda^2}{12} \mu\delta A^{n+1} \mu\delta f^{n+1} \\ &\quad = (1 + \delta^2/6)\, v^n - \frac{\lambda}{2} \mu\delta f^n + \frac{\lambda^2}{12} \mu\delta A^n \mu\delta f^n. \end{aligned} \tag{4.7a}$$

As in (2.9) we linearize this scheme around a second order accurate approximation $\hat{v}$ to v^{n+1}, and obtain

$$\begin{aligned} &\left(1 + \delta^2/6 + \frac{\lambda}{2} \mu\delta\hat{A} - \frac{\lambda^2}{12} \mu\delta\hat{A}\mu\delta\hat{A}\right) \Delta v^n \\ &\quad = -\frac{\lambda}{2} \mu\delta(f^n + \hat{f}) + \frac{\lambda^2}{12} \mu\delta(A^n \mu\delta f^n - \hat{A}\mu\delta\hat{f}) \equiv G^n, \end{aligned} \tag{4.7b}$$

where $\Delta v^n = v^{n+1} - v^n$. We denote this scheme by FP44.

We observe that FP44 differs from the compact CN44 only in the spatial discretization of the term $(Af_x)_x$. This modification removes the singularity due to the mesh oscillation eigenvector, thus allowing the use of larger time steps. The computational effort in setting up the matrix equation is the same. In [5] we have shown that one flux function f and one matrix function A have to be computed per mesh point per time step. However, pentadiagonal factorization is about 2.8 times more expensive than tridiagonal factorization ($N \gg 1$).

We see that the singularity in the coefficient matrix of CN44 can be removed at the cost of using a five-point scheme FP44. This involves not only more arithmetic operations but also an added complication in handling boundaries. We remark that FP44 can be generalized in a straightforward way to approximate the viscous equation

$$w_t + f(w)_x = \alpha w_{xx} \tag{4.8}$$

to fourth order accuracy. In this case five mesh points at each time level is the minimal number of points needed to achieve 4–4 accuracy.

In the next section we shall describe an iterative algorithm for FP44 which is more efficient than a direct LU factorization for $|\nu| \leqslant 4$. (Treatment of boundary conditions is discussed in [4].)

5. Iterative Algorithm for FP44

In this section we consider the following iterative algorithm for FP44,

$$\left(1 + \delta^2/6 + \frac{\lambda}{2}\mu\delta\hat{A}\right)(v^{(k+1)} - v^n) = G^n - \frac{\lambda^2}{12}\mu\delta\hat{A}\mu\delta\hat{A}(v^{(k)} - v^n), \qquad (5.1\text{a})$$

where

$$G^n = -\frac{\lambda}{2}\mu\delta(f^n + \hat{f}) + \frac{\lambda^2}{12}\mu\delta(A^n\mu\delta f^n - \hat{A}\mu\delta\hat{f}) \qquad (5.1\text{b})$$

and $v^{(0)}$ is some initial guess; usually $v^{(0)} = \hat{v}$. Observe that the coefficient matrix in (5.1a) is block tridiagonal and is identical in structure to that of CN24, except that it is computed at the state $\hat{v}$ rather than at v^n. This coefficnet matrix is always regular (see [4, Appendix A) and one can use a direct LU factorization without pivoting.

To study the convergence properties of this algorithm we do a Fourier analysis of the periodic scalar constant coefficient case.

$$\left(1 + \delta^2/6 + \frac{\nu}{2}\mu\delta\right)(v^{(k+1)} - v^n) = G^n - \frac{\nu^2}{12}(\mu\delta)^2(v^{(k)} - v^n), \qquad (5.2\text{a})$$

$$G^n = -\nu\mu\delta v^n, \qquad (5.2\text{b})$$

$\nu = \lambda A$ is the CFL number (1.3). Substituting $v_j^{(k)} = V^{(k)}e^{ij\xi}$, $v^n = V^n e^{ij\xi}$ (here $\xi = l\Delta x$ and l is the wave number) into (5.2) we obtain

$$\left(1 - \frac{2}{3}Y + \frac{\nu}{2}i\sin\xi\right)(V^{(k+1)} - V^n) = \mathscr{S}(G^n) + \frac{\nu^2}{3}Y(1-Y)(V^{(k)} - V^n), \quad (5.3\text{a})$$

$$\mathscr{S}(G^n) = -i\nu\sin\xi \cdot V^n. \qquad (5.3\text{b})$$

Thus, the algorithm (5.1) is convergent if and only if

$$|M(\xi,\nu)| \equiv \left|\frac{\nu^2 Y(1-Y)/3}{1 - \frac{2}{3}Y + (\nu/2)\,i\sin\xi}\right| = \frac{\nu^2 Y(1-Y)/3}{\sqrt{(1-\frac{2}{3}Y)^2 + \nu^2 Y(1-Y)}} < 1 \quad (5.3\text{c})$$

(see [8, pp. 61–64]); $Y = \sin^2(\xi/2)$, $0 \leqslant Y \leqslant 1$.

$|M(\xi,\nu)|$ obtains its maximal value $0.5 \leqslant Y \leqslant 0.581$. The following table shows the maximal value of $|M|$ as a function of $|\nu|$.

	$\lvert\nu\rvert$						
	0	1	2	3	4	5	6
$\max\lvert M\rvert$	0	0.10	0.29	0.46	0.63	0.80	0.97

(5.3d)

Thus, algorithm (5.1) is convergent for $|\nu| \leqslant 6$.

In the following we consider the algorithm (5.1) with the initial guess

$$v^{(0)} = \hat{v} = v^n - \lambda\mu\delta f^n + \frac{\lambda^2}{2}\delta A^n \delta f^n, \tag{5.4a}$$

i.e., $v^{(0)} = \hat{v}$ is computed by the Lax–Wendroff scheme. In this case $v^{(k)}$ for $k \geqslant 1$ is a fourth order accurate approximation to (1.1) as the term

$$\begin{aligned}\frac{\lambda^2}{12}\mu\delta\hat{A}\mu\delta[\hat{A}(\hat{v} - v^n) + \tilde{f}] &= \frac{\lambda^2}{12}\mu\delta\hat{A}\mu\delta\hat{f}\\ &= \frac{\lambda^2}{12}\mu\delta A^{n+1}\mu\delta f^{n+1} + O((\Delta t)^5).\end{aligned}$$

The amplification factor $S^{(1)}$ associated with the first iteration $v^{(1)}$ is given by

$$S^{(1)} = \frac{1 - \frac{2}{3}Y - i(\nu/2)\sin\xi + (\nu^2/3)\,Y(1 - Y)(\hat{S} - 1)}{1 - \frac{2}{3}Y + i(\nu/2)\sin\xi}, \tag{5.4b}$$

where $\hat{S}$ is the amplification factor of the Lax–Wendroff scheme in (5.4a), i.e.,

$$\hat{S} = 1 - i\nu\sin\xi - 2\nu^2 Y. \tag{5.4c}$$

The absolute value of $S^{(1)}$ is given by

$$|S^{(1)}|^2 = 1 - \frac{4}{9}\nu^4 Y^3(1 - Y)\cdot\frac{1 - \nu^2 Y(1 - Y)[(\nu^2 - 1)\,Y + 1]}{(1 - \frac{2}{3}Y)^2 + \nu^2 Y(1 - Y)}. \tag{5.4d}$$

It is easily seen that $|S^{(1)}| \leqslant 1$ for $|\nu| < \frac{3}{2}$; thus, the first iteration by itself constitutes a stable fourth order accurate scheme which is dissipative of order 6. For $|\nu| > \frac{3}{2}$ the first iteration is fourth order accurate but unstable by itself and we have to continue iterating in order to stabilize the algorithm.

In the following table we list k, the number of iterations needed per time-step, as a function of the CFL number. The data in this table is based on several scalar periodic variable coefficient and nonlinear test problems.

	$\lvert\nu\rvert$				
	1	1.5	2	3	4
k	1	1	2	3	7

(5.5)

We find that (5.1) is about

$$1+\frac{7k-5}{7m+5}$$

times more expensive than CN24, where m is the dimension of A in (1.2); e.g., for $m=3$ this factor is 1.35 and 1.62 for $k=2$ and $k=3$, respectively.

6. Two-Datum Representation of FP44

In this section we describe a two-datum representation of FP44. We introduce an additional auxiliary dependent variable p

$$p=\frac{\Delta t}{12}f(v)_x \tag{6.1a}$$

and a new state vector

$$W=\begin{pmatrix} p \\ v \end{pmatrix}; \tag{6.1b}$$

(Observe that $p=-(\Delta t/12)\,v_t$).

We now rewrite FP44 as the following system of two equations in p and v

$$\text{TD44:}\qquad (1+\delta^2/6)\,p^{n+1}-\frac{\lambda}{12}\mu\delta f(v^{n+1})=0, \tag{6.2a}$$

$$v^{n+1}+6p^{n+1}+\lambda\mu\delta(A^{n+1}p^{n+1})=v^n-6p^n+\lambda\mu\delta(A^np^n); \tag{6.2b}$$

as before $\lambda=\Delta t/\Delta x$.

The first equation, (6.2a), is the fourth order Padé spatial discretization (2.3b); the second equation, (6.2b), is the fourth order temporal discretization (2.7b). We denote the scheme (6.2a)–(6.2b) by TD44. Multiplying (6.2b) by the finite difference operator $(1+\delta^2/6)$ and then substituting $(1+\delta^2/6)\,p^k$, $k=n$ and $k=n+1$, from (6.2a), we see that TD44 is identical to FP44 in the constant coefficient case. TD44 differs from FP44 in the variable coefficient and the nonlinear case in terms containing derivatives of A, which are of the order of the truncation error (in the same way that the two-step schemes of Richtmyer and MacCormack differ from the Lax–Wendroff scheme).

We linearize TD44 in exactly the same way as in (2.9): let $\hat{v}$ be a second order accurate approximation to v^{n+1}, i.e.,

$$\hat{v} = v^{n+1} + O((\Delta t)^3) \tag{6.3a}$$

then

$$f^{n+1} = \hat{f} + \hat{A}(v^{n+1} - \hat{v}) + O((\Delta t)^6), \tag{6.3b}$$

$$A^{n+1} = \hat{A} + O((\Delta t)^3); \tag{6.3c}$$

and (6.2) becomes

$$12(1 + \delta^2/6)\, p^{n+1} + \lambda\mu\delta\hat{A} v^{n+1} = E^n, \tag{6.4a}$$

$$v^{n+1} + 6p^{n+1} + \lambda\mu\delta(\hat{A} p^{n+1}) = H^n, \tag{6.4b}$$

where

$$E^n = \lambda\mu\delta(\hat{f} - \hat{A}\hat{v}), \tag{6.4c}$$

$$H^n = v^n - 6p^n + \lambda\mu\delta(A^n p^n). \tag{6.4d}$$

The linearized scheme (6.4) can be written as the following block tridiagonal system of equations

$$\begin{pmatrix} 2 & \frac{\lambda}{2}\hat{A}_{j-1} \\ -\frac{\lambda}{2}\hat{A}_{j-1} & 0 \end{pmatrix} W_{j-1}^{n+1} + \begin{pmatrix} 8 & 0 \\ 6 & 1 \end{pmatrix} W_j^{n+1} + \begin{pmatrix} 2 & -\frac{\lambda}{2}\hat{A}_{j+1} \\ \frac{\lambda}{2}\hat{A}_{j+1} & 0 \end{pmatrix} W_{j+1}^{n+1} = \begin{pmatrix} E_j^n \\ H_j^n \end{pmatrix}. \tag{6.5}$$

It is to be understood that if A is an $m \times m$ matrix, then any scalar γ in (6.5) should be interpreted as $\gamma \cdot I_{m\times m}$, where $I_{m\times m}$ is a unit matrix of dimension m.

The compact three-point spatial discretization in TD44 makes it possible to accommodate boundary conditions with relative ease (see [4]). Initial and boundary values for p are derivable from corresponding values for v via the definition (6.1a) and the partial differential equation (1.1).

Perhaps the most attractive feature of TD44 is its algorithmic simplicity: only H^0 has to be computed by (6.4d). For all $n \geqslant 1$ we compute H^n by

$$H^n = H^{n-1} - 12P^n. \tag{6.6a}$$

This recursive relation, (6.6a), follows from (6.4b), (6.4d) and the observation

$$\lambda\mu\delta(\hat{A}p^{n+1}) = \lambda\mu\delta(A^{n+1}p^{n+1}) + O((\Delta t)^5).$$

We have already mentioned that $\hat{v} = v^{n+1} + O((\Delta t)^3)$ need not be obtained by a stable approximation. A convenient way to compute $\hat{v}$ is given by

$$\hat{v} = 5v^n + 24p^n + 6H^{n-1}. \tag{6.6b}$$

This relation is derived from the Taylor expension

$$\hat{v} = w^n + \Delta t w_t^n + \frac{(\Delta t)^2}{2} w_{tt}^n + O((\Delta t)^3) = v^n + 12p^n + 6\lambda\mu\delta(A^n p^n)$$

and the substitution $\lambda\mu\delta(A^n p^n) = H^{n-1} - v^n - 6P^n$ from (6.4b).

We remark that the term $\hat{f} - \hat{A}\hat{v}$ in E^n (6.4c) should be computed analytically as it represents a linearization error and therefore a significant reduction in the operational count is to be expected. Some physical systems governed by conservation laws, e.g., the Eulerian equations of gas dynamics, have the property that the nonlinear vector [redacted]

$$f \equiv Av, \tag{6.7}$$

where as before A is the Jacobian of f with respect to v. It follows from (6.7) that in this case $E^n \equiv 0$ for all n. The TD44 algorithm is particularly simple for conservation laws with an homogeneous flux (e.g., Eulerian equations of gas dynamics). To advance the solution in one time step we execute the following algorithm:

(i) Calculate

$$H^n = H^{n-1} - 12p^n, \tag{6.7a}$$

(ii) Calculate

$$\hat{v} = -5v^n + 24p^n + 6H^n, \tag{6.7b}$$

(iii) Evaluate $\hat{A} = A(\hat{v})$,

(iv) Solve the block tridiagonal system (6.5).

In such a case $A(v)$ is typically a matrix with easy to compute entries; clearly the major part of the computational effort is to solve the block tridiagonal system of Eq. (6.5).

The blocks in (6.5) are of dimension $2m$, twice as large as that of CN24 and FP44; however, out of 12 entries in the three coefficient matrices in (6.5), three are zero and five are scalar times identity. To take full advantage of this structure as well as the structure of the matrix A, it seems advisable to use iterative methods for the solution of (6.5). (An accelerated Gauss–Seidel iteration of a two-datum representation of CN22 and CN24 is presented in [12]).

7. Variable Coefficient Problems

In this section we consider a hyperbolic variable coefficient problem of the form

$$w_t + A(x)\, w_x = 0. \tag{7.1}$$

In this case $w_t = -A(x)\, w_x$, $w_{tt} = A(x)[A(x)\, w_x]_x$, therefore the time discretization formula (2.7a) becomes

$$w^{n+1} + \frac{\Delta t}{A} A(x)\, w_x^{n+1} + \frac{(\Delta t)^2}{12} A(x)[A(x)\, w_x^{n+1}]_x \tag{7.2a}$$

$$= w^n - \frac{\Delta t}{2} A(x)\, w_x^n + \frac{(\Delta t)^2}{12} A(x)[A(x)\, w_x^n]_x + O((\Delta t)^5). \tag{7.2a}$$

To obtain fourth order accuracy in the spatial discretization we approximate the term $(\Delta t/2)\, A(x)\, w_x$ in (7.2a) by a modified Padé formula

$$A(x)\, w_x = \frac{1}{3\Delta x} \frac{4\mu A\delta - A\mu\delta}{1 + \delta^2/6}\, w + O((\Delta x)^4), \tag{7.2b}$$

and just as before it is sufficient to approximate the higher order term $((\Delta t)^2/12)\, A(x)[A(x)\, w_x]_x$ by

$$A(x)[A(x)\, w_x]_x = \frac{1}{(\Delta x)^2} A\mu\delta A\mu\delta w + O((\Delta x)^2). \tag{7.2c}$$

Rearranging terms we get the following Δ-formulation for CN22 (2.6a), CN24 (2.6b) and FP44 (4.7b)

$$\left[1 + \alpha_{2-4}\delta^2/6 + \frac{\lambda}{6}(4\mu A - A\mu)\,\delta + \alpha_{4-4}\frac{\lambda^2}{12} A\mu\delta A\mu\delta\right] \Delta v^n$$
$$= -\frac{\lambda}{3}(4\mu A - A\mu)\,\delta v^n, \tag{7.3}$$

where FP44 is given by $\alpha_{2-4} = \alpha_{4-4} = 1$, CN24 is given by $\alpha_{2-4} = 1$, $\alpha_{4-4} = 0$ and CN22 is given by $\alpha_{2-4} = \alpha_{4-4} = 0$.

Next we describe some numerical experiments with the periodic, scalar, variable coefficient problem

$$w_t + \frac{1}{2 + \cos x}\, w_x = 0, \qquad -\pi \leqslant x \leqslant \pi, \quad t \geqslant 0 \tag{7.4a}$$

with the initial data

$$w(x, 0) = 2 + \sin(2x + \sin x) \qquad -\pi \leqslant x \leqslant \pi \tag{7.4b}$$

and the periodic boundary conditions

$$w(-\pi, t) \equiv w(\pi, t), \qquad t \geqslant 0. \tag{7.4c}$$

The exact solution to the problem (7.4a)–(7.4c) is

$$w(x, t) = 2 + \sin(2x + \sin x - t). \tag{7.4d}$$

In Table I we present a mesh refinement chart for CN22, CN24 and FP44. It shows the relative l_2-error in sequences of calculations with a fixed CFL number ν

$$\nu = \frac{\Delta t}{\Delta x} \max_{-\pi \leqslant x \leqslant \pi} |A(x)|; \qquad \Delta x = 2\pi/N, \tag{7.5}$$

in which the number of grid points N and the number of time steps n are successively doubled. For comparison we show refinement sequences for $\nu = 1, 2, 4$.

In Table II we show the dependence of the error on the CFL number ν in a fixed

TABLE I

Mesh Refinement Chart – Variable Coefficient Problem (7.4)

CFL	Time	n	N	CN22	Ratio	CN24	Ratio	FP44	Ratio
1.	6.28	20	20	2.07×10^{-1}		2.18×10^{-2}		7.27×10^{-3}	
					3.73		4.70		17.07
		40	40	5.55×10^{-2}		4.63×10^{-3}		4.26×10^{-4}	
					3.96		4.17		16.20
		80	80	1.40×10^{-2}		1.11×10^{-3}		2.63×10^{-5}	
					3.99		4.04		16.13
		160	160	3.52×10^{-3}		2.75×10^{-4}		1.63×10^{-6}	
2.	12.57	20	20	4.43×10^{-1}		1.40×10^{-1}		2.26×10^{-2}	
					3.38		3.90		16.62
		40	40	1.31×10^{-1}		3.51×10^{-2}		1.36×10^{-3}	
					3.97		4.00		16.00
		80	80	3.30×10^{-2}		8.77×10^{-3}		8.50×10^{-5}	
					4.01		4.00		16.01
		160	160	8.23×10^{-3}		2.19×10^{-3}		5.31×10^{-6}	
4.	25.13	20	20	5.05×10^{-1}		6.43×10^{-1}		1.32×10^{-1}	
					1.24		2.49		14.68
		40	40	4.06×10^{-1}		2.58×10^{-1}		8.99×10^{-3}	
					3.50		3.73		15.72
		80	80	1.16×10^{-1}		6.91×10^{-2}		5.72×10^{-4}	
					3.93		3.95		15.93
		160	160	2.95×10^{-2}		1.75×10^{-2}		3.59×10^{-5}	

TABLE II

Dependence on CFL Number – Variable Coefficient Problem (7.4)

CFL	Time	n	N	CN22	Ratio	CN24	Ratio	FP44	Ratio
1.	25.13	320	80	5.29×10^{-2}		4.45×10^{-3}		8.91×10^{-5}	
					1.24		3.93		1.91
2.	25.13	160	80	6.58×10^{-2}		1.75×10^{-2}		1.70×10^{-4}	
					1.76		3.95		3.36
4.	25.13	80	80	1.16×10^{-1}		6.91×10^{-2}		5.72×10^{-4}	
					2.56		3.72		5.94
8.	25.13	40	80	2.97×10^{-1}		2.57×10^{-1}		3.40×10^{-3}	

mesh calculation. The relative l_2-error used in Tables I, II, and all subsequent tables is defined by

$$E_2(v) = \left[\frac{\sum (v_j - w_j)^2}{\sum w_j^2} \right]^{1/2}, \tag{7.6}$$

where v_j is the numerical solution and w_j is the exact solution.

We make the following observations regarding the data in Tables I and II:

(1) FP44 is indeed fully fourth order accurate: a refinement by a factor of 2 reduces the error by a factor of approximately $16 = 2^4$.

(2) CN22 exhibits a very poor accuracy, even in relatively fine meshes (e.g., 5.6% error with 40 mesh points for $\sin(2x + \sin x)$, $-\pi \leqslant x \leqslant \pi$, in one period of time-oscillation).

(3) CN24 is considerably more accurate than CN22 for CFL numbers smaller or equal to 1 (see [5]); however, it is only negligibly more accurate for CFL numbers around 4. The 4–4 schemes are always considerably more accurate than CN24, e.g., FP44 with $n = N = 40$ in Table I is as accurate as CN24 with $n = N = 160$; FP44 with $n = 40$, $N = 80$ and $\nu = 8$ in Table II is more accurate than CN24 with $n = 320$, $N = 80$ and $\nu = 1$.

(4) $\nu \approx 0.25$ seems to be the optimal choice for CN24 (see [5, 11]); $\nu \approx 2.5$ seems to be the optimal choice for FP44.

8. NONLINEAR PROBLEMS

In this section we examine numerical solutions to the nonlinear conservation law (1.1). FP44 (4.7b) is linearized around a solution of the one-step Lax–Wendroff scheme, i.e.,

$$\hat{v} = v^n - \lambda\mu\delta f^n + \frac{\lambda^2}{2}\delta A^n \delta f^n. \tag{8.1}$$

First, we describe numerical experiments with the following periodic scalar problem

$$w_t + \left(\frac{w^2}{2}\right)_x = 0, \qquad -\pi \leqslant x \leqslant \pi, \quad t \geqslant 0 \tag{8.2a}$$

with the initial data

$$w(x, 0) = d + \sin x, \qquad d = \text{const.}, \quad -\pi \leqslant x \leqslant \pi, \tag{8.2b}$$

and the periodic boundary conditions

$$w(-\pi, t) \equiv w(\pi, t), \qquad t \geqslant 0. \tag{8.2c}$$

It is easy to see that for all values of d the solution to (8.2) is smooth up to $t = 1$, at which time a shock wave begins to form. After formation this shock decays at a fast rate which is typical of periodic problems (see [4, Appendix B].

In Table III we present a mesh refinement chart for numerical solutions of CN22,

TABLE III

Mesh Refinement Chart—Nonlinear Problem (8.2)

CFL	Time	n	N	CN22	Ratio	CN24	Ratio	FP44	Ratio
1.	0.628	12	40	7.92×10^{-3}		1.98×10^{-3}		4.59×10^{-4}	
					3.62		4.00		12.57
		24	80	2.19×10^{-3}		4.95×10^{-4}		3.65×10^{-5}	
					3.88		4.02		15.21
		48	160	5.65×10^{-4}		1.23×10^{-4}		2.40×10^{-6}	
					3.98		3.98		15.89
		96	320	1.42×10^{-4}		3.09×10^{-5}		1.51×10^{-7}	
2.	0.628	6	40	1.18×10^{-2}		6.75×10^{-3}		1.14×10^{-3}	
					3.41		3.59		9.83
		12	80	3.46×10^{-3}		1.88×10^{-3}		1.16×10^{-4}	
					3.79		3.86		13.68
		24	160	9.15×10^{-4}		4.87×10^{-4}		8.48×10^{-6}	
					3.93		3.96		15.45
		48	320	2.33×10^{-4}		1.23×10^{-4}		5.49×10^{-7}	
4.	0.628	3	40	2.44×10^{-2}		2.07×10^{-2}		4.50×10^{-3}	
					3.05		3.09		7.34
		6	80	8.01×10^{-3}		6.70×10^{-3}		6.13×10^{-4}	
					3.53		3.58		11.54
		12	160	2.27×10^{-3}		1.87×10^{-3}		5.31×10^{-5}	
					3.83		3.84		14.79
		24	320	5.93×10^{-4}		4.87×10^{-4}		3.59×10^{-6}	

CN24 and FP44 to (6.3) with $d = 2$. The time-step $\Delta t^{(n)}$ in these calculations is calculated at each time level by

$$\frac{\Delta t^{(n)}}{\Delta x} \max_j |A(v_j^n)| = \nu, \qquad \Delta x = 2\pi/N, \tag{8.3}$$

where v_j^n is the FP44 solution and ν is the fixed CFL number. The l_2 errors (7.6) in this table correspond to $t = 0.628$, at which the solution is still smooth.

Table III shows that FP44 is indeed a fully fourth order accurate scheme. The fact that the Lax–Wendroff scheme (8.1) is unstable for $|\nu| > 1$ does not seem to effect the stability of FP44 for $|\nu| > 1$. The relation between the error of CN22, CN24 and FP44 is about the same as in the variable coefficient case (Tables I, II). All the schemes in Table III exhibit a deterioration of accuracy with increasing CFL numbers which is much stronger than in the variable coefficient case. This is to be expected as in the nonlinear case, there is an additional linearization error which increases with the CFL number.

FP44, as well as CN22 and CN24, is a nondissipative scheme and therefore it is susceptible to nonlinear instabilities, e.g., CN22, CN24, and FP44, when applied to (8.2) with $d = 0$, develop a strong nonlinear instability after the formation of a stationary shock at $t = 1$ at the boundaries $x = \pm\pi$ (see [5] and the references cited there). To prevent such occurrences, as well as to improve calculations with shocks, we supplement these schemes with an external dissipation mechanism in the form of a switched Shuman filter F (see [7]). Let L denote our finite difference scheme (CN22, CN24, or FP44 in this case), and let $\tilde{v} = Lv^n$ be the numerical solution at the advanced time level. We now consider the dissipative scheme

$$\begin{cases} \tilde{v} = Lv^n \\ v^{n+1} = F\tilde{v} \end{cases} \qquad \text{or} \qquad v^{n+1} = \tilde{L}v^n \equiv (FL)\, v^n, \tag{8.4a}$$

where

$$(F\tilde{v})_j = \tilde{v}_j + \frac{\alpha}{4} \left[\theta_{j+1/2}(\tilde{v}_{j+1} - \tilde{v}_j) - \theta_{j-1/2}(\tilde{v}_j - \tilde{v}_{j-1})\right]; \tag{8.4b}$$

θ is an automatic switch, $0 \leqslant \theta \leqslant 1$. Observe that when $\theta_{j+1/2} \equiv 1$ and $\alpha = 1$, F is the averaging operator, $F = \mu^2$, $\mu = \frac{1}{2}(T^{-1/2} + T^{1/2})$. Fourier analysis of (8.4b) under the assumption $\theta_{j+1/2} \equiv \theta = \text{const}$, $0 \leqslant \theta \leqslant 1$, shows that $\|F\|_2 \leqslant 1$ for $0 \leqslant \alpha \leqslant 2$. Thus, if L is stable so is $\tilde{L}$.

We apply (8.4) with the following automatic switch θ

$$\theta_{j+1/2} = \frac{|\delta^k \Delta\sigma(\tilde{v})_j|}{|\delta|^k\, |\Delta\sigma(\tilde{v})_j|}, \tag{8.5a}$$

where $\delta = T^{1/2} - T^{-1/2}$, $|\delta| = T^{1/2} + T^{-1/2} = 2\mu$, $\Delta = T - I$ and $\sigma(\tilde{v})$ is some function of $\tilde{v}$. It follows immediately from its definition that

$$0 \leqslant \theta_{j+1/2} \leqslant 1, \tag{8.5b}$$

and that

$$\theta_{j+1/2}(\tilde{v}_{j+1} - \tilde{v}_j) = O((\Delta x)^{k+1}) \tag{8.5c}$$

wherever $\tilde{v}$ is sufficiently smooth. Hence, choosing $k = R$ in (8.5), where R is the order of accuracy of L, guarantees that $\tilde{L}$ (8.4) has the same formal order of accuracy as L. We demonstrate this point in Table IV by repeating the calculations in Table III using $\tilde{L}$ rather than L, with $k = 2$ for CN22 and $k = 4$ for CN24 and FP44; $\alpha = 1$ and $\sigma(v) \equiv v$ in (8.4)–(8.5).

We turn now to describe the performance of CN22, CN24 and FP44 in calculating [illegible] [10]). This is self evident from the fact that all the terms in (2.6a)–(2.6b) and (4.7b), except for Δv^n, have a δ operator in front of them (note that $\mu\delta = \delta\mu$). The switched Shuman filter F in (8.4) is also in conservation form (see [7]). The conservation form is of particular significance in computing shocks as it guarantees correct propagation of shock fronts (see [10]).

In Figs. 1–4 we show solutions of CN22, CN24, and FP44 to the periodic problem (8.2) with $d = 2$. Figure 1 shows the results after 80 time-steps with $\nu = 1$ and $N = 40$

TABLE IV

Mesh Refinement Chart—Nonlinear Problem (8.2) with Shuman Filter

CFL	Time	n	N	CN22	Ratio	CN24	Ratio	FP44	Ratio
1.	0.628	10	40	8.39×10^{-3}		2.11×10^{-3}		6.91×10^{-4}	
					3.65		4.20		12.00
		24	80	2.30×10^{-3}		5.02×10^{-4}		5.76×10^{-5}	
					3.95		4.05		17.56
		48	160	5.83×10^{-4}		1.24×10^{-4}		3.28×10^{-6}	
					4.02		4.01		18.02
		96	320	1.45×10^{-4}		3.09×10^{-5}		1.82×10^{-7}	
2.	0.628	6	40	1.20×10^{-2}		6.80×10^{-3}		1.25×10^{-3}	
					3.43		3.62		10.08
		12	80	3.50×10^{-3}		1.88×10^{-3}		1.24×10^{-3}	
					3.79		3.86		14.03
		24	160	9.23×10^{-4}		4.87×10^{-4}		8.84×10^{-5}	
					3.94		3.96		15.79
		48	320	2.34×10^{-4}		1.23×10^{-4}		5.0×10^{-6}	
4.	0.628	3	40	2.44×10^{-2}		2.07×10^{-2}		4.54×10^{-3}	
					3.04		3.09		7.37
		6	80	8.03×10^{-3}		6.70×10^{-3}		6.16×10^{-4}	
					3.54		3.58		11.56
		12	160	2.27×10^{-3}		1.87×10^{-3}		5.33×10^{-5}	
					3.83		3.84		14.85
		24	320	5.93×10^{-4}		4.87×10^{-3}		3.59×10^{-6}	

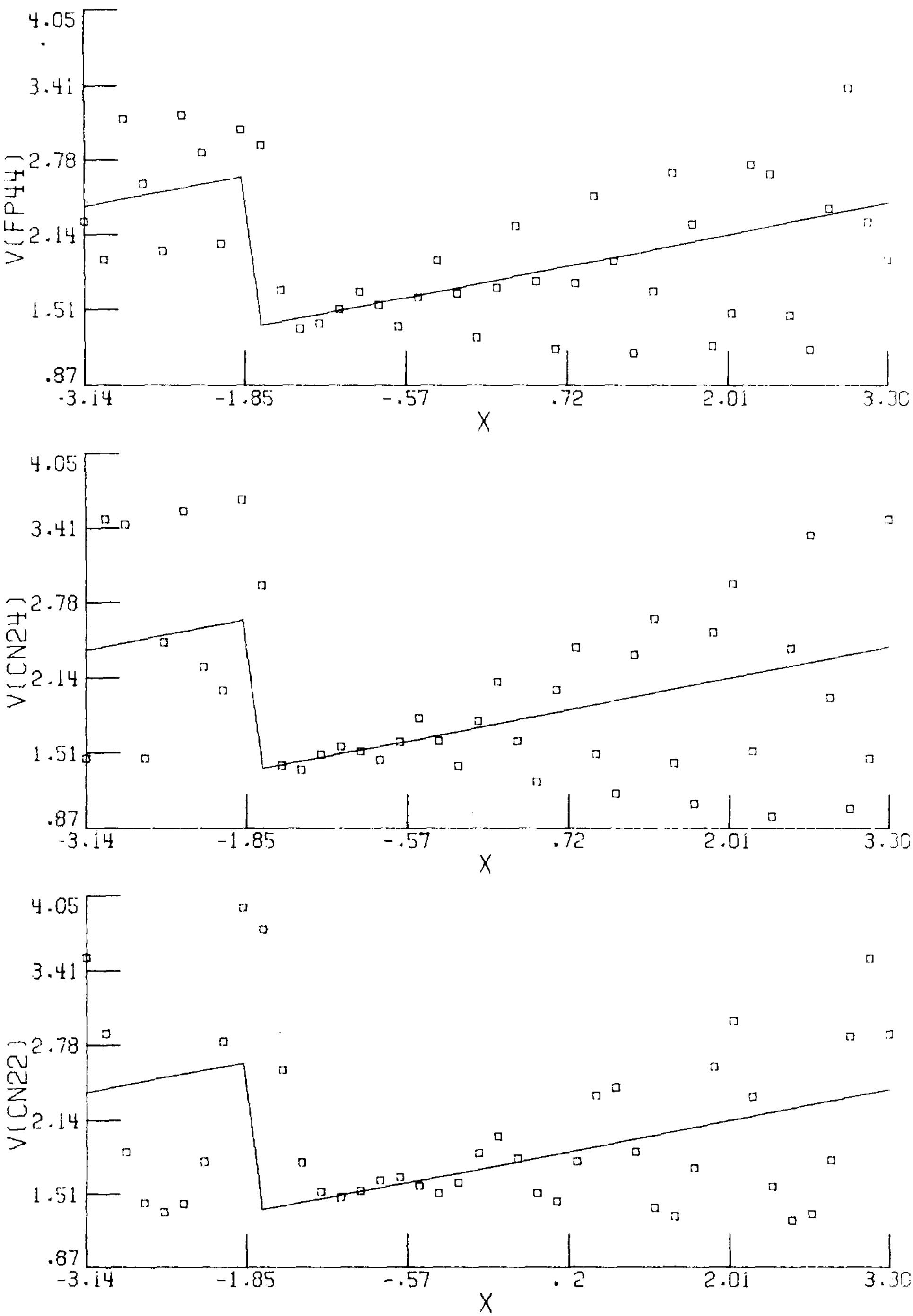

FIG. 1. Solutions to (8.2) for $\nu = 1$ and no filtering ($t = 3.80$, $n = 80$).

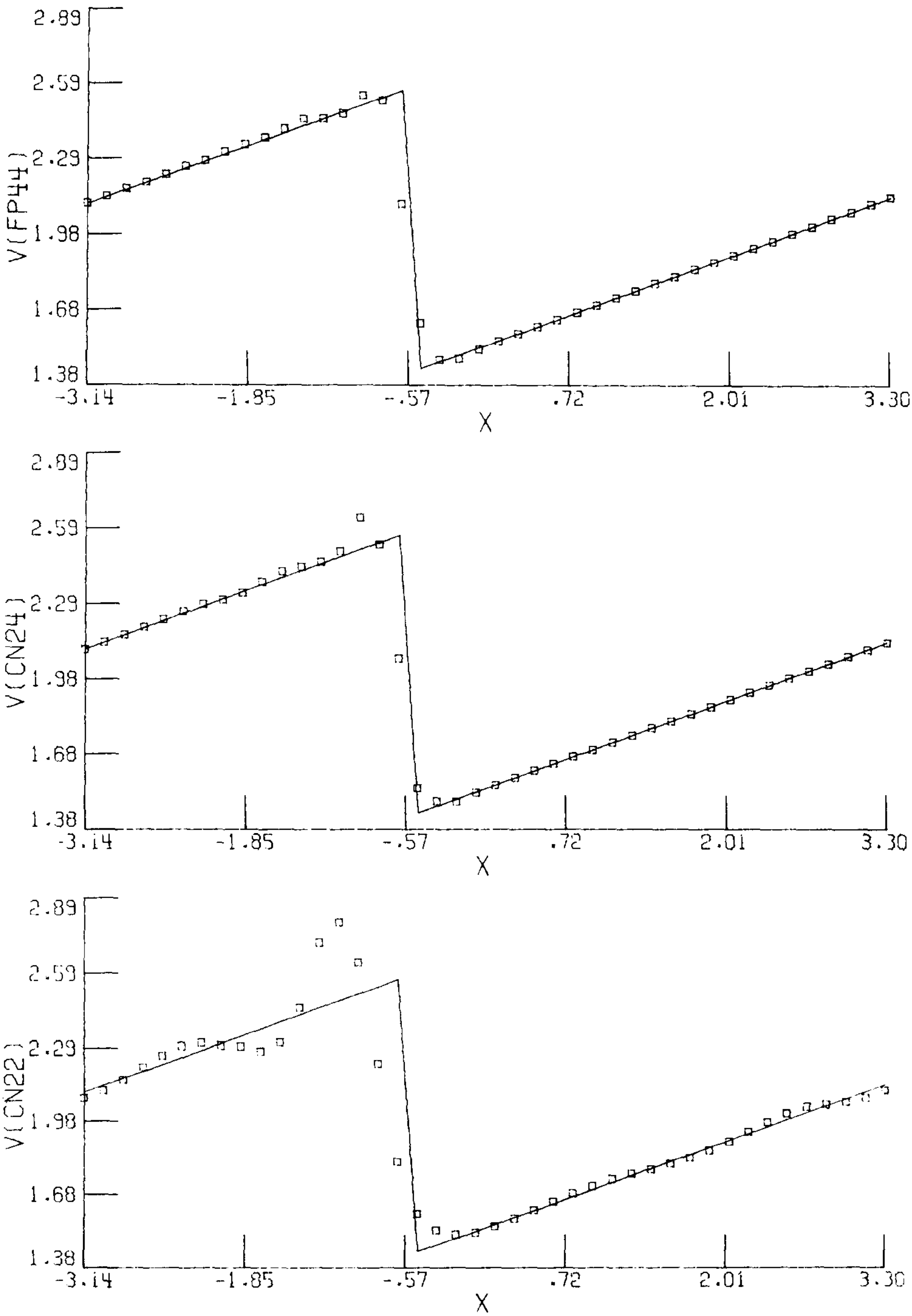

FIG. 2. Solutions to (8.2) for $\nu = 1$ with Shuman filtering ($t = 4.43$, $n = 80$).

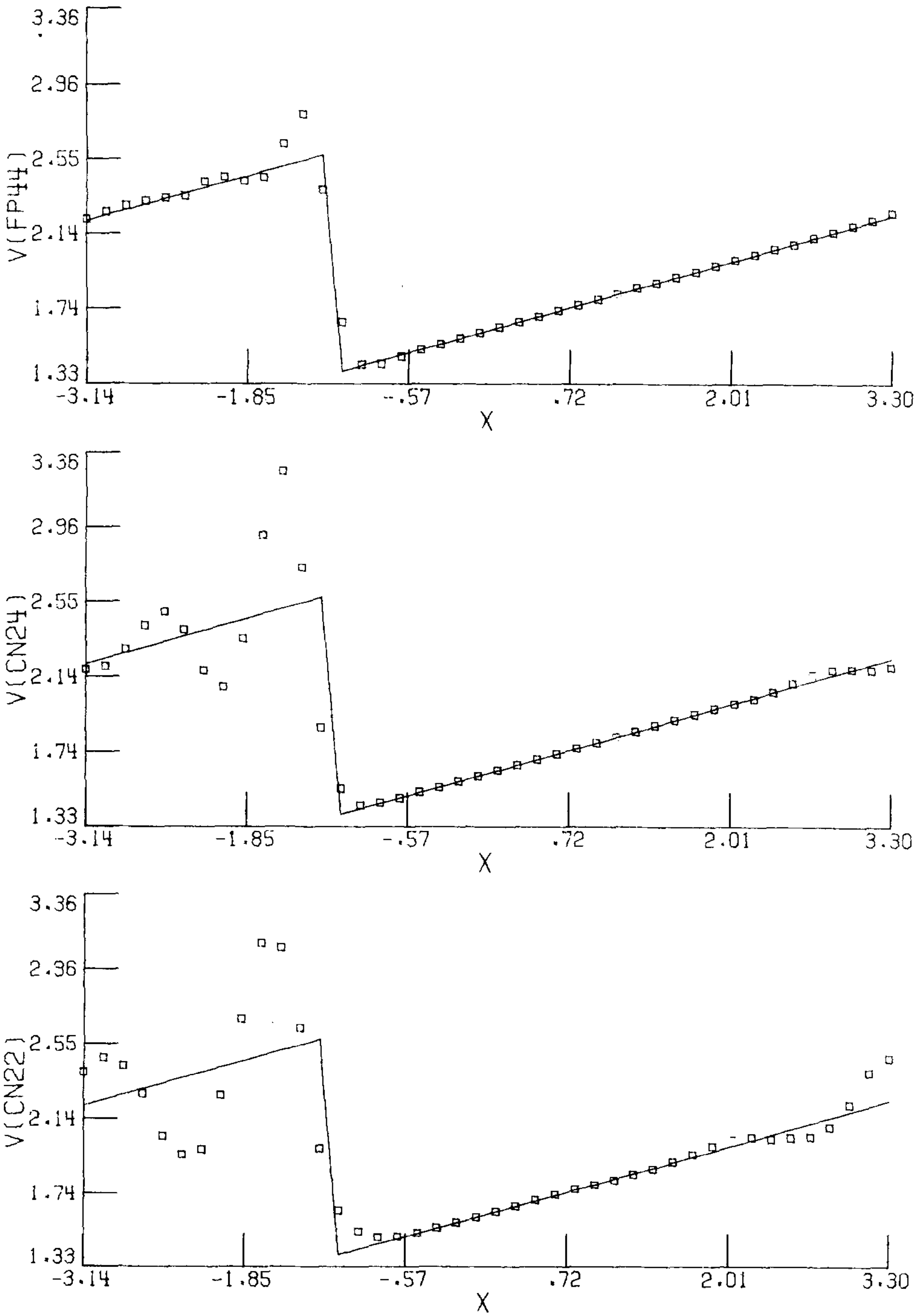

FIG. 3. Solutions to (8.2) for $\nu = 2$ with Shuman filtering ($t = 4.16$, $n = 40$).

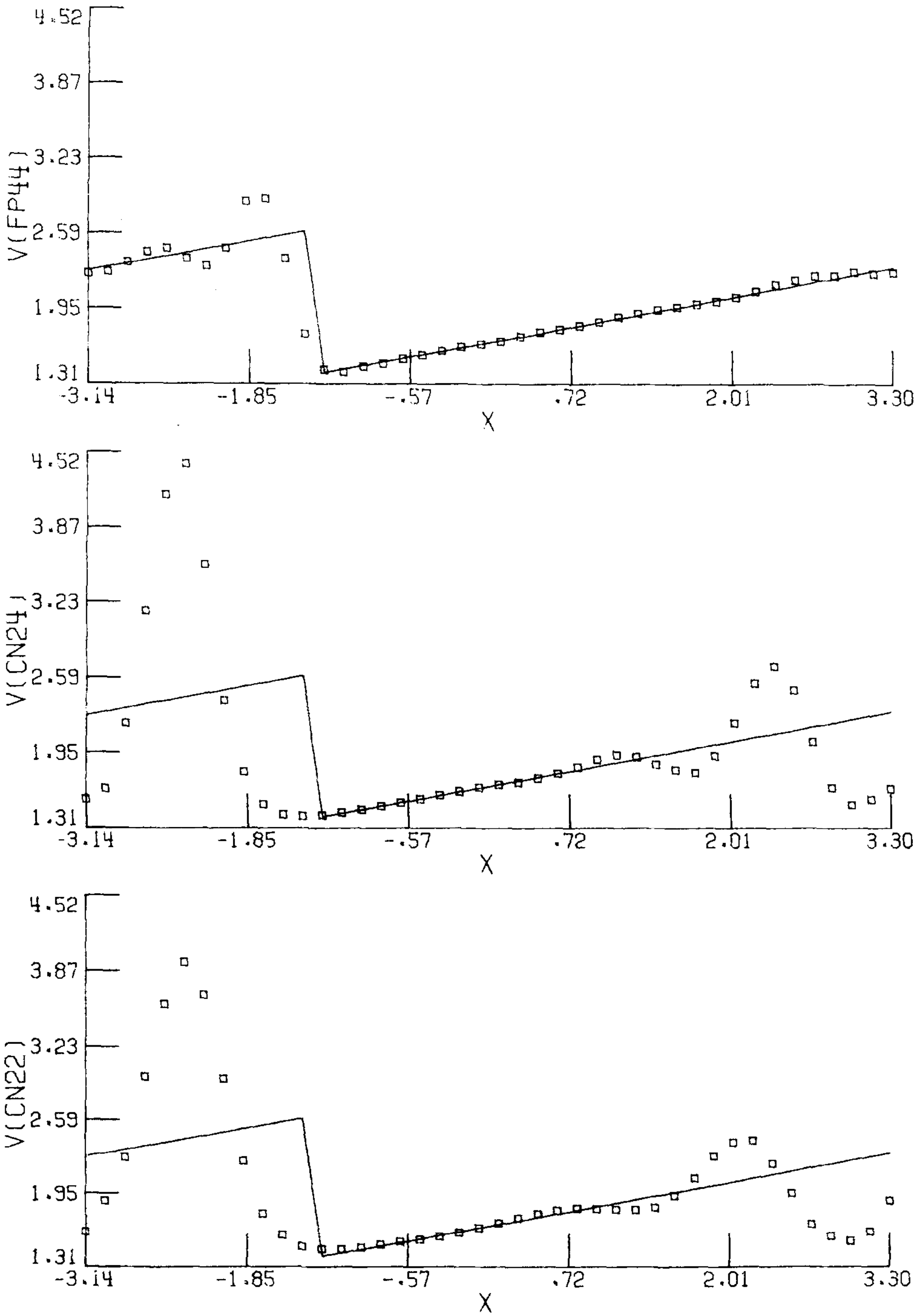

FIG. 4. Solutions to (8.2) for $\nu = 4$ with filtering ($t = 4.03$, $n = 20$).

in (8.3). The solutions in Fig. 1 are oscillating to the point of being meaningless. In Fig. 2 we repeat this calculation with $\tilde{L}$ where $a = 2$ and $\sigma(v) \equiv v$ in (8.4)–(8.5). The solutions of CN24 and FP44 are now rather accurate but the solution of CN22 is still oscillating. In Figs. 3 and 4 we demonstrate that when shocks are present there is no sense in going to CFL numbers much larger than 1. In Fig. 3 we repeat the calculation of Fig. 2 with 40 time-steps and $\nu = 2$. Figure 4 shows the results with 20 time-steps and $\nu = 4$; here we have to apply the switched Shuman filter twice at each time-step, i.e., $\tilde{L} = F^2 L$, as well as to filter $\hat{v}$ in (8.1), to obtain stable results for FP44.

Next we describe numerical experiments with the following Riemann problem (shock tube) for the Eulerian equation of a polytropic gas:

$$w_t + f(w)_x = 0, \tag{8.6a}$$

$$w = \begin{pmatrix} \rho \\ m \\ E \end{pmatrix}, \qquad f(w) = uw + \begin{pmatrix} 0 \\ P \\ Pu \end{pmatrix},$$

$$P = (\gamma - 1)(E - \tfrac{1}{2}\rho u^2), \tag{8.6b}$$

$$w(x, 0) = \begin{Bmatrix} w_L & x \leqslant 0 \\ w_R & x > 0 \end{Bmatrix}, \qquad w_L = \begin{pmatrix} 1 \\ 0. \\ 2.5 \end{pmatrix}, \qquad w_R = \begin{pmatrix} 0.125 \\ 0. \\ 0.25 \end{pmatrix}. \tag{8.6c}$$

Here ρ, u, P and E are the density, velocity, pressure and total energy, respectively; $m = \rho u$ is the momentum, $\gamma = 1.4$. The exact solution of this Riemann problem consists of a shock propagating to the right followed by a contact discontinuity, and a left propagating rarefaction wave. This exact solution is shown in Figs. 5 and 6 by a continuous line.

The flux $f(w)$ in (8.6a) is a homogeneous function of the components of w, i.e., $f(w) \equiv Aw$. The linearization (2.9) becomes

$$f^{n+1} = \hat{f} + \hat{A}(v^{n+1} - \hat{v}) + O((\Delta t)^6) = \hat{A} v^{n+1} + O((\Delta t)^6). \tag{8.7}$$

Figure 5 shows the solution of (8.6) with the 4–4 scheme

$$\left(1 + \delta^2/6 + \frac{\lambda}{2}\mu\delta\hat{A}\right) v^{n+1} = (1 + \delta^2/6)\, v^n - \frac{\lambda}{2}\mu\delta f^n + \frac{\lambda^2}{12}\mu\delta(A^n\delta f^n - \hat{A}\delta\hat{f}) \tag{8.8a}$$

with

$$\hat{v} = v^n - \lambda\mu\delta f^n + \frac{\lambda^2}{2}\delta A^n \delta f^n. \tag{8.8b}$$

This scheme is a simplified form of (5.1a) with $k = 1$ and $\hat{v}^{(0)}$ given by the Lax–Wendroff scheme (5.4a). We saw in Section 5 that (8.8) is stable and dissipative for $|\nu| < 1.5$. Fig. 5 shows the solution of the Riemann problem (8.6) for 50 time-steps under the restriction $|\nu| \leqslant 1$, obtained by the scheme (8.8). At the end of each time-

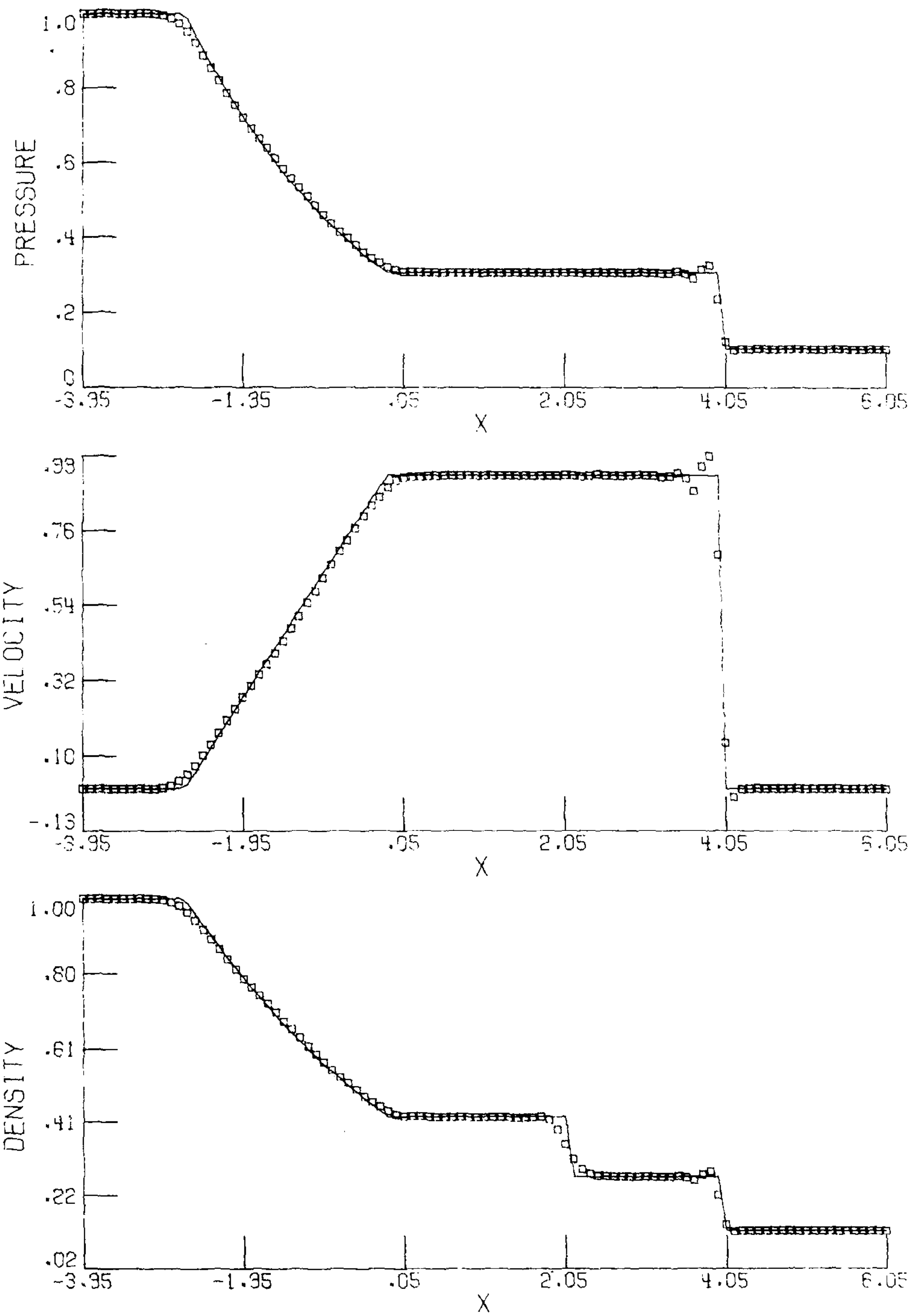

FIG. 5. Solution of the 4–4 scheme (8.8) to the Riemann Problem (8.6).

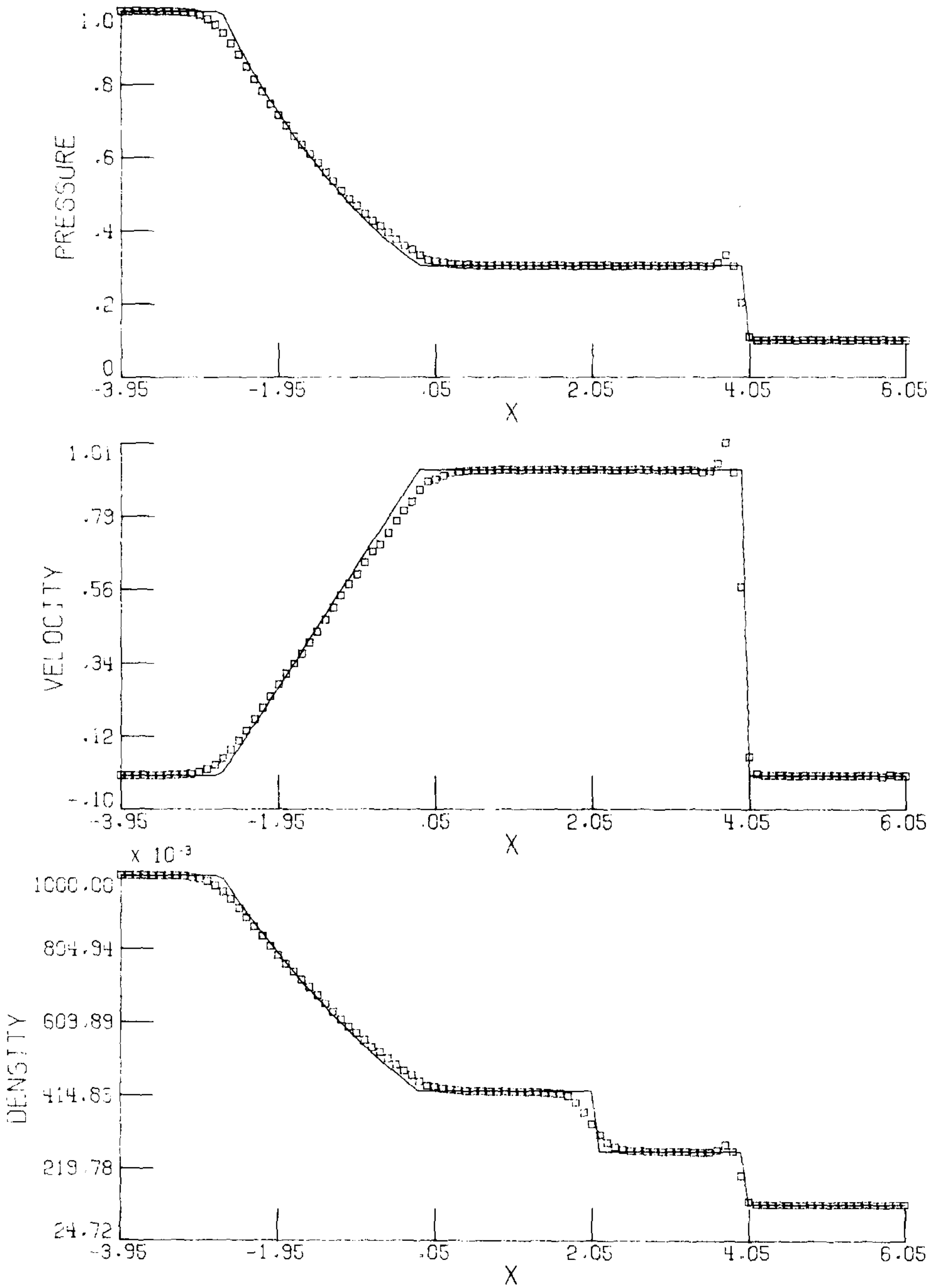

FIG. 6. Solution of CN24 to the Riemann Problem (8.6).

step, the numerical solution is filtered by applying (8.4b) with $\alpha = 1$ and $\sigma(v) = \rho$, $k = 4$ in (8.5a).

For comparison we show in Fig. 6 the same calculation with CN24, except that here we take $\alpha = 2$ in the Shuman filter to account for the nondissiptivity of CN24.

We conclude that CN22, CN24 and FP44 with Shuman filtering can handle shocks, provided that the CFL number is not much larger than 1. Hybridization techniques (see [6]) may produce better results for higher CFL numbers.

ACKNOWLEDGMENTS

We thank Alvin Bayliss, Eugene Isaacson, Dan Marchesin and Gideon Zwas for many helpful and stimulating discussions.

REFERENCES

1. R. M. BEAM AND R. F. WARMING, *J. Comput. Phys.* **22** (1976), 87–110.
2. R. M. BEAM AND R. F. WARMING, AIAA J. **16** (1978), 393–402.
3. P. DAVIS AND P. RABINOWITZ, "Methods of Numerical Integration," Academic Press, New York, 1974.
4. A. HARTEN AND H. TAL-EZER, On a fourth order accurate implicit finite difference scheme for hyperbolic conservation laws. II. Five point schemes, ICASE Report No. 79–10, NASA Langley Research Center, June 1979.
5. A. HARTEN AND H. TAL-EZER, On a fourth order accurate implicit finite difference scheme for hyperbolic conservation laws. I. Nonstiff strongly dynamic problems, ICASE Report No. 79-1, NASA Langley Research Center, January 1979.
6. A. HARTEN AND G. ZWAS, *J. Comput. Phys.* **9** (1972), 568–583.
7. A. HARTEN AND G. ZWAS, *J. Eng. Math.* **6** (1972), 207–216.
8. E. ISAACSON AND H. KELLER, "Analysis of Numerical Methods," Wiley, New York, 1966.
9. A. JAMESON AND E. TURKEL, Implicit schemes and LU decompositions, to appear.
10. P. D. LAX AND B. WENDROFF, *Comm. Pure Appl. Math.* **23** (1960), 217–237.
11. E. TURKEL, *J. Comput. Phys.* **35** (1980), 319–340.
12. H. J. WIRZ, F. DESCHUTTER, AND A. TURI, *Math. Comput. Simulation* **19** (1977), 241–261.